Superconducting transition at 38 K in insulating-overdoped $La_2CuO_4 - La_{1.64}Sr_{0.36}CuO_4$ superlattices: Evidence for interface electronic redistribution from resonant soft x-ray scattering

S. Smadici,[1] J. C. T. Lee,[1] S. Wang,[1] P. Abbamonte,[1] G. Logvenov,[2] A. Gozar,[2] C. Deville Cavellin,[2,3] and I. Bozovic[2]

[1] *Frederick Seitz Materials Research Laboratory, University of Illinois, Urbana, IL 61801, USA*
[2] *Brookhaven National Laboratory, Upton, NY 11973, USA*
[3] *Université Paris 12, 94010 Créteil Cedex, France*

arXiv:0805.3189v2 [cond-mat.str-el] 13 Feb 2009

We use resonant soft x-ray scattering (RSXS) to quantify the hole distribution in a superlattice of insulating La_2CuO_4 (LCO) and overdoped $La_{2-x}Sr_xCuO_4$ (LSCO). Despite its non-superconducting constituents, this structure is superconducting with $T_c = 38$ K. We found that the conducting holes redistribute electronically from LSCO to the LCO layers. The LCO layers were found to be optimally doped, suggesting they are the main drivers of superconductivity. Our results demonstrate the utility of RSXS for separating electronic from structural effects at oxide interfaces.

PACS numbers: 74.78.-w, 74.72.-h, 73.21.-b

The interface between two correlated electron systems can exhibit ground states that are not stable in the bulk of either of its constituents. This tendency could provide a novel route to new devices. [1, 2, 3, 4, 5] An interesting realization of this idea are the two-dimensional electron gases (2DEGs) observed at the interfaces between $LaTiO_3$ and $SrTiO_3$[6], $SrTiO_3$ and $LaAlO_3$[7, 8], $LaMnO_3$ and $SrMnO_3$[9, 10, 11], La_2CuO_4 and $La_{2-x}Sr_xCuO_4$[12, 13], and ZnO and $Mg_xZn_{1-x}O$[14], which exhibit phenomena ranging from magnetoresistance to the quantum Hall effect to superconductivity.

One of the outstanding questions in this field is whether the 2DEGs observed in these heterostructures are truly 'intrinsic' interface properties that arise from charge accumulation, or if they simply arise from defects like oxygen vacancies or cation interdiffusion. These two effects are virtually impossible to distinguish with transport measurements alone.

In this paper we present a quantitative study, using resonant soft x-ray scattering (RSXS), of the charge distribution in a superlattice of insulating La_2CuO_4 (LCO) and overdoped $La_{1.64}Sr_{0.36}CuO_4$ (LSCO). Despite its nonsuperconducting constituents, this heterostructure is superconducting with $T_c = 38$ K. [13] Using RSXS, a technique that can probe the holes independently of the atomic lattice, we find that the hole density varies more gradually than the distribution of Sr^{2+} cations, indicating redistribution of carriers among the layers. Applying a linear response model, we show that this redistribution takes place over a characteristic distance of $\lambda_0 = 6.1 \pm 2.0$ Å. The LCO layers are found to be highly doped, with filling $p = 0.18$ holes/Cu, suggesting that superconductivity arises in the 'insulating' substructure. Our results show that genuine charge accumulation can be achieved in oxide heterostructures, and can be observed with RSXS.

Superlattices with LCO and LSCO sublayers of various thicknesses were grown in a unique atomic layer-by-layer MBE (ALL-MBE) system on $LaSrAlO_4$ (LSAO) substrates. Structures were monitored during growth with time-of-flight ion scattering and recoil spectroscopy (TOF-ISARS) and reflection high-energy electron diffraction (RHEED). The samples were annealed to remove any excess, interstitial oxygen. The single-phase overdoped LSCO has in-plane lattice constants almost the same (to within 0.03 %) as the LSAO substrate. LCO layers are strained, but even under maximal strain single-phase LCO remains insulating and not superconducting. The sample selected for RSXS studies consisted of 15 repeats of 2 × LCO + 4 × LSCO, which despite its non-superconducting constituents had $T_c = 38$ K, [13] close to the value for optimally doped LSCO crystals. Hard x-ray measurements (Fig. 1b, blue line) were done on a reflectometer. X-ray absorption (XAS) measurements (Fig. 2b, square symbols) showed the sample to be highly doped on average, with a small peak at the upper Hubbard band (UHB) that is seen more clearly in the resonance profile (red symbols).

RSXS measurements were done at the undulator beam line X1B at the National Synchrotron Light Source in an ultra-high vacuum (UHV) diffractometer. Measurements were made in the specular geometry, i.e. in reflectivity mode, with the momentum transfer perpendicular to the plane of the superlattice. Momenta will be written in terms of the third Miller index L, i.e. $Q = 2\pi L/c$, where $c = 39.84$ Å is the superlattice period. The X1 undulator produces both horizontally and vertically polarized light in the proportions $P_\pi = 0.93$ and $P_\sigma = 0.07$, defined by the orientation with respect to the scattering plane (Fig. 1a, inset). The detector integrated over both scattering channels. XAS measurements were done *in situ* in fluorescence yield mode. The incident energy resolution was set to $\Delta E = 0.2$ eV, and all measurements were done at $T = 90$ K which was found to eliminate radiation damage.

Initial RSXS measurements are summarized in Fig. 1b,

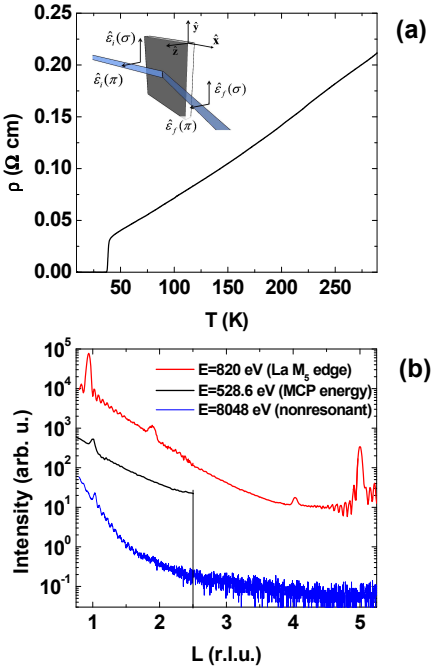

FIG. 1: (color online) (a). Superlattice resistivity showing T_c = 38.4 K. (Inset) Experimental geometry showing the direction of incident and scattered polarizations. (b). Specular x-ray reflectivity measurements as a function of L (blue) off resonance, (red) near the La M_5 edge, and (black) at the mobile carrier peak (MCP) below the O K edge. At the La M_5 edge the peaks are slightly shifted from the integer values because of refraction effects. Thickness oscillations are visible, indicating flat interfaces. The width of the $L = 1$ peak is determined by the thickness of the superlattice. The $L = 2$ reflection is visible at the La edge, but not at the MCP, indicating that the holes do not follow the profile of Sr dopants.

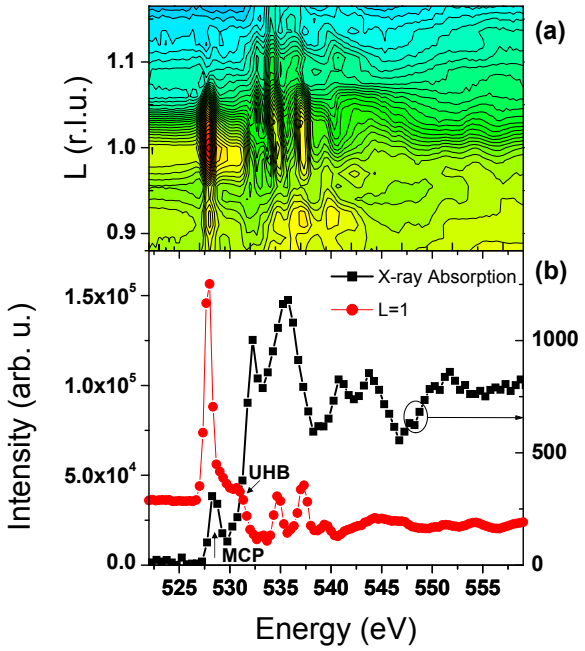

FIG. 2: (color online) Energy dependence of the $L = 1$ superlattice reflection near the O K edge. (a). Color plot (logarithmic color scale), showing that the reflection is enhanced at the energy of the mobile carrier prepeak (MCP), which indicates that the holes are modulated with the period of the superlattice. (b). Summary plot comparing the intensity of the $L = 1$ reflection from (a) (red circles), to the x-ray absorption spectrum (black squares). The slight energy shift between the XAS and resonance maximum occurs because of interference between resonant and off-resonant scattering. This interference allows us to determine quantitatively the amplitude of the hole modulation.

which shows the scattered intensity as a function of L for various photon energies. The data are rather featureless far from resonance (8048 eV). Near the La M_5 edge (820 eV) however, several peaks are visible at integer L, which are reflections from the superlattice period [15]. The reason these are visible at the La edge is that the contrast between LCO and LSCO layers, which have different La content, is enhanced. The relative intensities of these peaks are determined by the profile of Sr dopants in the superlattice.

The scattering of x-rays from the doped holes, which reflects their distribution, is enhanced if the beam energy is tuned to the mobile carrier peak (MCP) below the O K edge [16, 17] (Fig. 2b, arrow). In Figs. 2a and 2b (red circles) we show scattering near this energy (528.6 eV). A giant resonance is visible near $L = 1$, indicating that, as expected, the holes are modulated with the period of the superlattice. [18] In contrast to scattering at the La edge, however, no peak is visible at $L = 2$ for scattering at the MCP energy. (Fig. 1b) This shows that the distribution of holes does not exactly follow that of the Sr atoms. Suppression of a harmonic, in fact, suggests that the hole density varies more gradually than the profile of the Sr^{2+} ions, which is evidence for redistribution of holes among the layers.

The hole distribution can be determined quantitatively from this scattering. The integrated intensity of the charge reflection at momentum L is given by

$$\frac{I_L}{AV} = P_\sigma |\hat{\epsilon}_f^*(\sigma) \cdot \mathbf{S}_L \cdot \hat{\epsilon}_i(\sigma)|^2 + P_\pi |\hat{\epsilon}_f^*(\pi) \cdot \mathbf{S}_L \cdot \hat{\epsilon}_i(\pi)|^2 \quad (1)$$

where $\mathbf{S}_L$ is the structure factor tensor, $\hat{\epsilon}_f$ and $\hat{\epsilon}_i$ are final and initial polarization states (defined as in Fig. 1a, inset), V is the scattering volume, and A contains all proportionality factors, e.g. beam intensity, unit cell volume, etc. The σ term must be included since, although P_σ is small, $\hat{\epsilon}_{i,f}(\sigma)$ lie in the CuO_2 plane so this scattering has a large resonant enhancement.

The structure factor comprises two terms $\mathbf{S}_L = \mathbf{S}_L^0 + \mathbf{S}_L^D$. The first term

$$(\mathbf{S}_L^0)_{ij} = \delta_{ij} \sum_{l,n} d_l^n \, f_n(\omega) \, e^{i2\pi L z_l / c} \quad (2)$$

is the lattice structure factor, which is isotropic and describes scattering from the atomic lattice. Here z_l is the

position of layer l, d_l^n is the number of atoms of type n in one $a \times a$ area of this layer, and $f_n(\omega)$ is the scattering factor of atom type n. [19] The matrix d_l^n defines the structure of the superlattice, including the distribution of defects. For clarity we will first analyze our data assuming a perfect structure, and correct the result for defects afterward.

The second term

$$(\mathbf{S}_L^D)_{ij} = f_{ij}^D(\omega) \sum_l \frac{p_l^0}{2} e^{i2\pi L z_l/c} \tag{3}$$

is anisotropic and describes scattering from the doped holes. p_l^0 is the hole count per Cu atom in layer l in an ideal structure, and $f_{ij}^D(\omega)$ is the scattering power of a doped hole. [16, 20] The factor 1/2 accounts for the fact that there are two planar oxygen atoms for each Cu atom.

We wish to determine p_l^0, which is the distribution of holes in the superlattice. This task is simplified by realizing that, by symmetry (Fig. 3b), our structure has only three inequivalent CuO_2 planes: the two central LSCO layers, the two outer LSCO layers, and the two LCO layers. We denote the hole occupancies in these layers by p_{max}^0, p_{int}^0 and p_{min}^0, respectively (see labels in Fig. 3b). Further, by charge conservation, it must be that $p_{max}^0 + p_{min}^0 + p_{int}^0 = 0.72$ holes. Therefore, to completely determine the hole distribution in this superlattice, we need only two more independent measurements of these three values.

The first measurement is the scattering near $L = 2$. Written out, the structure factor of this reflection is

$$(\mathbf{S}_2)_{ij} = 0.84\, x [f_{La}(\omega) - f_{Sr}(\omega)]\, \delta_{ij} +$$

$$+0.5(p_{min}^0 + p_{max}^0 - 2p_{int}^0) f_{ij}^D(\omega) \tag{4}$$

where $x = 0.36$ is the doping of the LSCO layers. The origin $z = 0$ was chosen between two LCO layers. This reflection is not visible off-resonance, but becomes visible near the La M_5 edge because the difference $f_{La}(\omega) - f_{Sr}(\omega)$ becomes large. However, near the MCP resonance, where f_{ij}^D is large (164 electrons at the resonance maximum [16]), the peak is not observed. That it is absent is evidence that it is forbidden by symmetry, i.e. $p_{max}^0 + p_{min}^0 - 2p_{int}^0 \approx 0$. With the constraint of charge conservation this gives $p_{int}^0 \approx 0.24$. The nominal doping of this layer is 0.36 holes, so this result shows – prior to knowledge of p_{max}^0 and p_{min}^0 – that holes have diffused from the interface layer.

The second measurement comes from the scattering near $L = 1$. The structure factor of this reflection is

$$(\mathbf{S}_1)_{ij} = 1.66\, x [f_{Sr}(\omega) - f_{La}(\omega)]\, \delta_{ij} +$$

$$+0.87\, (p_{max}^0 - p_{min}^0) f_{ij}^D(\omega). \tag{5}$$

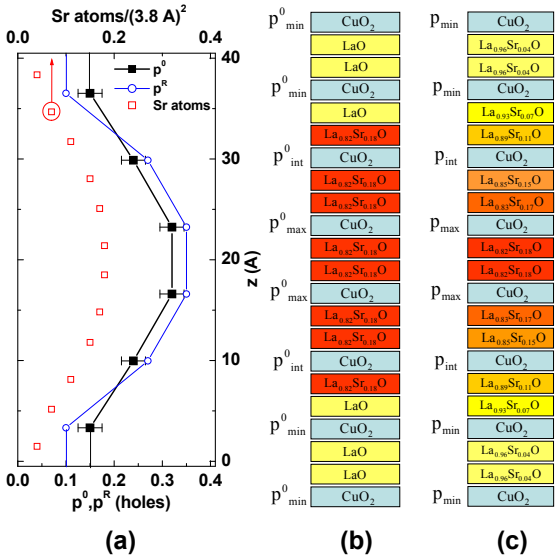

FIG. 3: (color online) (a) Layer-resolved hole count in an ideal structure (solid squares) and the hole count that would obtain from structural roughness only (open circles). These two distributions are convolved to achieve the hole distribution in the real structure (panel c). The error bars represent our uncertainty in determining P_σ and P_π in Eq. 1, as well as statistical errors. Also shown is the nominal distribution of Sr^{2+} ions (open squares). (b) Sketch of the superlattice hole distribution in an ideal structure, aligned to panel (a) for comparison. (c) Sketch of the hole distribution in the real structure, accounting for La/Sr interdiffusion. p_{min}^0 and p_{min}^R are the hole counts in the LCO layers contributed by electronic effects and by roughness, respectively.

Unlike the $L = 2$ reflection, this peak is visible at both the La M_5 and MCP resonances, indicating that it is allowed by symmetry, i.e. the difference $p_{max}^0 - p_{min}^0$ is nonzero. Knowledge of this difference would completely determine the hole distribution in the superlattice.

To determine $p_{max}^0 - p_{min}^0$ directly from this reflection, however would require a measurement of $\mathbf{S}_1$ in absolute units, i.e. the knowledge of the overall constant A in Eq. 1, whose value derives from many different effects. We can eliminate A, however, by noting that f_{ij}^D quickly goes to zero away from the resonance energy [16], and that the remaining terms f_{La} and f_{Sr} are tabulated [21]. $p_{max}^0 - p_{min}^0$ can therefore be determined from the relative increase in intensity of $L = 1$ scattering at MCP from that a few eV below the edge. [22] A detailed energy dependence of $L = 1$ scattering is shown in Fig. 2. From the relative increase in integrated intensity at MCP of 560 %, and using the method outlined above to eliminate A, we obtain $p_{max}^0 - p_{min}^0 = 0.18$. From these constraints we calculate $p_{max}^0 = 0.33 \pm 0.025$ and $p_{min}^0 = 0.15 \pm 0.025$.

This result is significant because it shows that the carriers are not bound to the Sr^{2+} ions, but rearrange between layers, presumably to minimize their kinetic energy. For the perfect structure (roughness effects will be

considered below) the "undoped" LCO layers have a hole count of at least 0.15 holes/Cu, which is close to optimal doping for the LSCO system. This suggests that superconductivity originates in the nominally insulating LCO layers.

Having determined the hole distribution, it is useful to characterize it with a screening length, λ_0. The simplest way to define λ_0 is in linear Thomas-Fermi theory, relating the charge ρ^{ind} induced in a medium to the external charge density ρ^{ext} by

$$\rho^{ind}(Q) = -\frac{k_0^2}{k_0^2 + Q^2}\,\rho^{ext}(Q), \qquad (6)$$

where $k_0 = 1/\lambda_0$ is the Thomas-Fermi wave vector.

In the present case the "external" charge is that of the Sr^{2+} ions [23], and the induced charge is the hole occupancy p_l^0, i.e. $\rho^{ext}(Q) = \sum_l d_l^{Sr}\, e^{iQz_l}$ and $\rho^{ind}(Q) = \sum_l p_l^0\, e^{iQz_l}$, where d_l^{Sr} and p_l^0 were defined in Eqs. 2-3. For the $L = 1$ reflection, for which $Q = 2\pi/c$, $\rho^{ext} = -1.66\,x$ and $\rho^{ind} = 1.73\,(p^0_{max} - p^0_{min})$, resulting in $\lambda_0 = 6.1 \pm 2.0$ Å. This would be the characteristic size of the accumulation region in a device made of these two materials.

We now consider the effect of interfacial roughness on the previous conclusions. The structure is not perfect, but contains step edges from island formation during growth [13], as well as some La-Sr interdiffusion. For specular measurements such defects can be modeled well by a convolution of the La-Sr profile with a Gaussian roughness function. From convolution theorem this correction enters as a multiplicative factor in momentum space $R(Q) = e^{-Q^2\sigma^2/2}$, where σ is the interface roughness. This factor has the effect of suppressing higher order reflections. From the ratio of the $L = 1$ and $L = 2$ reflections at the La edge, we determine $\sigma = 5.3$ Å. This roughness causes a smearing of the hole density *in addition* to the electronic redistribution we have already shown. Including roughness, the structure factor at $L = 1$ is modified as

$$(\mathbf{S}_1)_{ij} = 1.66\,x[f_{Sr}(\omega) - f_{La}(\omega)]\,\delta_{ij}\,R(2\pi/c) +$$

$$+0.87\,(p_{max} - p_{min}) f_{ij}^D(\omega), \qquad (7)$$

where p_{max} and p_{min} are the actual hole occupancies in the real, imperfect structure. From Eq. 6 it follows that $p_{max} - p_{min} = (p^0_{max} - p^0_{min})R(2\pi/c)$. Thus in our earlier analysis, in which S_1^D was determined by normalizing to the value of S_1^0, the term $R(2\pi/c)$ divided out. As a result, the method used above to obtain λ_0 is independent of roughness effects. Further, the quantities $p^0_{max} = 0.33$, $p^0_{int} = 0.24$ and $p^0_{min} = 0.15$ can be thought of as those that would have obtained if the structure were defect-free. Including the roughness contribution, the true p values in our structure are $p_{max} = 0.30 \pm 0.03$, $p_{int} = 0.24 \pm 0.03$ and $p_{min} = 0.18 \pm 0.03$. We note that, if we include only the roughness, the values are $p^R_{max} = 0.35$, $p^R_{int} = 0.27$ and $p^R_{min} = 0.10$. p^R is defined as the CuO_2 layer doping due solely to the roughness of the structure. Therefore, the dominant cause of doping of LCO layers is electronic accumulation, not defects.

In conclusion, we have used RSXS to quantify the distribution of holes in a superlattice of insulating LCO and nonsuperconducting LSCO. We find that the distribution of holes differs from that of the Sr^{2+} ions, indicating true charge accumulation. The filling of the LCO layers is found to be close to 0.18 holes/Cu, suggesting that the 'insulating' layers are the main drivers of superconductivity. Our study demonstrates that charge accumulation can be achieved at transition metal oxide interfaces with existing synthesis methods. Our study also demonstrates the usefulness of RSXS for distinguishing atomic from electronic reconstruction at transition metal oxide interfaces.

This work was supported by the Office of Basic Energy Sciences, U.S. Department of Energy. RSXS studies were supported by Grant No. DE-FG02-06ER46285, with use of the NSLS supported under Contract No. DE-AC02-98CH10886. Superlattice growth and characterization were supported under Contract No. MA-509-MACA. Work in the FSMRL was supported by grants DE-FG02-07ER46453 and DE-FG02-07ER46471.

[1] S. Okamoto and A. J. Millis, Nature **428**, 630 (2004).
[2] S. Okamoto, A. J. Millis, and N. A. Spaldin, Phys. Rev. Lett. **97**, 56802 (2006).
[3] S. Altieri, L. H. Tjeng, G. A. Sawatzky, Thin Solid Films **400**, 9 (2001).
[4] R. Pentcheva and W. E. Pickett, Phys. Rev. Lett. **99**, 016802 (2007).
[5] J. Chakhalian *et al.*, Science **318**, 1114 (2007).
[6] A. Ohtomo *et al.*, Nature **419**, 378 (2002).
[7] N. Reyren *et al.*, Science **317**, 1196 (2007).
[8] A. Ohtomo and H. Y. Hwang, Nature **427**, 423 (2004).
[9] A. Bhattacharya *et al.*, arXiv:0710.1452.
[10] T. Koida *et al.*, Phys. Rev. B **66**, 144418 (2002).
[11] S. Smadici *et al.*, Phys. Rev. Lett. **99**, 196404 (2007).
[12] I. Bozovic *et al.*, Phys. Rev. Lett. **93**, 157002 (2004).
[13] A. Gozar *et al.*, Nature **455**, 782 (2008).
[14] A. Tsukazaki *et al.*, Science **315**, 1388 (2007).
[15] The $L = 3$ reflection is always absent by symmetry. This may readily be verified by evaluating Eqs. 2-3.
[16] P. Abbamonte *et al.*, Nature Physics **1**, 155 (2005).
[17] P. Abbamonte *et al.*, Science **297**, 581 (2002).
[18] No change in the intensity of the $L = 1$ reflection was seen across the superconducting transition temperature.
[19] This quantity is equivalent to the "raw" scattering factor defined in Ref. [16].
[20] P. Abbamonte, Phys. Rev. B **74**, 195113 (2006).
[21] B.L. Henke, E. M. Gullikson, and J. C. Davis, At. Nucl. Data Tables **54**, 181 (1993).
[22] The quantities A, f_{La} and f_{Sr} are all in principle energy-

dependent. However they do not change appreciably between 520 eV and 530 eV.
[23] Technically the sum includes all charged layers. However, only the Sr^{2+} ions enter for $L = 1$.